Electronic Supplementary Material (ESI) for Nanoscale.

Electronic Supplementary Information

Blue, Green, and Red Full-Color Ultralong Afterglow in Nitrogen-Doped Carbon Dots

Cunjian Lin, Yixi Zhuang,* Wuhui Li, Tian-Liang Zhou, and Rong-Jun Xie*

College of Materials, Xiamen University, Simingnan-Road 422, Xiamen, 361005 P.R. China

Table of Contents

Section I. Chemicals and Materials

Folic acid (FA), ethyl alcohol (EtOH), ethidene diamine (EDA), and urea were purchased from Sinopharm Chemical Reagent Corporation. Dimethyl formamide (DMF), *o*-phenylenediamines (oPD), and biuret were obtained from Aladdin Corporation. All the chemical reagents in this work were used as received without further purification.

Section II. Synthesis and Preparation

Synthesis of NCD1. FA (1 g) was dispersed in EtOH (30 mL). After stirring for 10 min, the solution was transferred into a Teflon-lined autoclave (100 mL), heated at 260 °C for 2 h, and cooled down to room temperature (RT) naturally. Dark crude product was obtained by centrifugation in 11000 rpm for 10 min. The precipitates were dried under vacuum at 80 °C for 6 h. Subsequently, 50 mg of the obtained product was dispersed in 10 mL deionized (DI) water with ultrasonic waves for 10 min. The dark brown solution was centrifuged at 11000 rpm for 5 min to remove agglomerated particles. The crude products of NCD1 were further dialyzed against DI water in a dialysis bag (500D) for 2 days to remove unreacted reagents and small molecular species. The supernatant containing NCD1 was collected for further use.

Synthesis of NCD2. NCD2 was synthesized using a previously reported method with some modifications.[1] FA (0.3 g) was dissolved in DI water (30 mL). After stirring for 10 min, the solution was transferred into a Teflon-lined autoclave (100 mL), heated at 260 °C for 2 h, and cooled down to room temperature (RT) naturally. The obtained dark solution was centrifuged under 11000 rpm for 10 min to remove agglomerated particles. NCD2 was separated from the solution by frozen-drying at -50 ºC. The unreacted reagent, small molecular species, and solution were all removed. And NCD2 was redispersed in DI water (120 mL) with ultrasonic waves for 10 min. An aqueous solution containing NCD2 (~5 mg/mL) was obtained for further use.

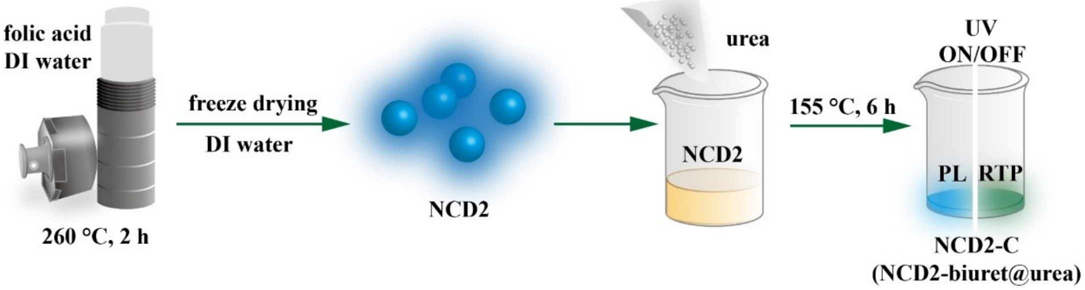

Scheme S1. Schematic illustration for the preparations of NCD2 and NCD2-C.

Synthesis of NCD3. oPD (0.3 g) was firstly dissolved in EtOH (30 mL). After stirring for 10 min, EDA (300 μL) was added into the solution. The solution was transferred into a Teflon-lined autoclave (100 mL) and heated at 180 °C for 12 h, using a previously reported method with some modifications.[2] The reactors were cooled down to RT naturally after the hydrothermal reaction. The crude product was dialyzed against DI water in a membrane tube [molecular weight cut-off (MWCO) of 500] for 2 days to remove unreacted reagent and small molecular species. The NCD3 was collected inside the membrane tube.

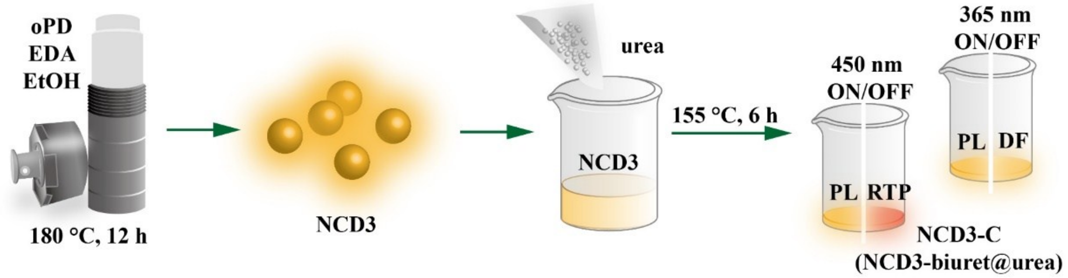

Scheme S2. Schematic illustration for the preparations of NCD3 and NCD3-C.

Synthesis of NCDs-biuret@urea composites. 3 mL of NCD1, NCD2, or NCD3 solution was mixed with urea aqueous solution (1 g/mL). After stirring for 10 min, the mixed solutions were transferred into a beaker, and heated at 155 °C for 6 h in an oven. NCDs-biuret@urea composites (~4.0 g) with long afterglow feature were obtained after the heating reaction.[3]

Preparation of anti-counterfeiting inks. The obtained NCDs-biuret@urea composites (~4.0 g) were dissolved in DMF (10 mL) with ultrasonic waves for 20 min. Anti-counterfeiting inks with ultrahigh solid solubility and excellent dispersion stability were obtained.

Section III. Characterizations

Transmission electron microscopy (TEM) and high resolution TEM (HR-TEM) images of the NCDs were observed in JEM-2100F (JEOL), which was operated at an accelerating voltage of 200 kV. All the AFM measurements were obtained using a Cypher S AFM (Asylum Research/Oxford Instruments, Santa Barbara, CA). X-ray diffraction (XRD) patterns were carried out by using a XRD-7000 X-ray diffractometer from Shimadzu Corporation, Japan. The Raman spectra were performed by using the IDSpec ARCTIC Raman system. Fourier transform infrared (FT-IR) spectra were recorded in Nicolet iS10 (Thermo Scientific). X-ray photoelectron spectroscopy (XPS) was analyzed in 250Xi (ESCALAB). Fluorescence and afterglow spectra were recorded by using a spectrometer F-4600 (Hitachi). UV-vis absorption spectra were measured on a spectrophotometer UV-3600-plus (Shimadzu). Fluorescent decay curves and Afterglow decay curves were obtained in a spectrometer FLS 980 (Edinburgh Instrument). Fluorescence quantum yield (QY) at RT was tested by using an absolute QY spectrometer (Hamamatsu, C11347). The afterglow QY was measured by using FS5 (Edinburgh Instrument). TGA experiments were carried out on a TG209F1 thermal analyzer under air atmosphere from

RT to 260 °C with a heating rate of 10 °C/min. The anti-counterfeiting inks were printed by using an inkjet printer DeskJet 1112 (HP). The electric input powers of the 254, 365, and 450 nm lamps are 10, 10, and 2 W, respectively. The illuminance areas of these light sources are 15 * 4, 15 * 4, and 2.5 * 2.5 cm^2. Paper with lower FL intensity (compared with common office paper), supplied by Sanyecao Corporation, was used for printing. Photographs of the inks in quartz or printed on paper were recorded by a digital camera (Canon, EOS 5D MarkII) equipped with a lens (Canon, EF 50 mm f/2.8 Macro). Movies were recorded by using a digital camera (Canon, EOS 700D) equipped with a lens (Canon, EF 50 mm f/1.8 STM).

Section IV. Supporting Figures and Tables

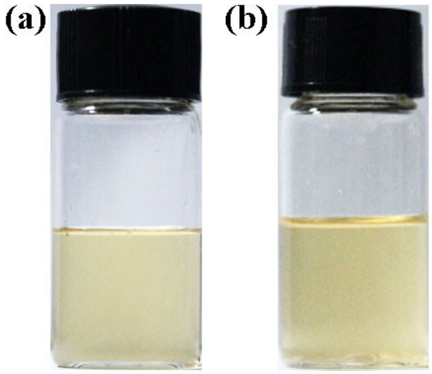

Figure S1. Photographs of NCD1-C anti-counterfeiting ink. (a) is a fresh ink and (b) is an ink preserved at RT for six months. No obvious variation (ink color and optical properties) could be observed.

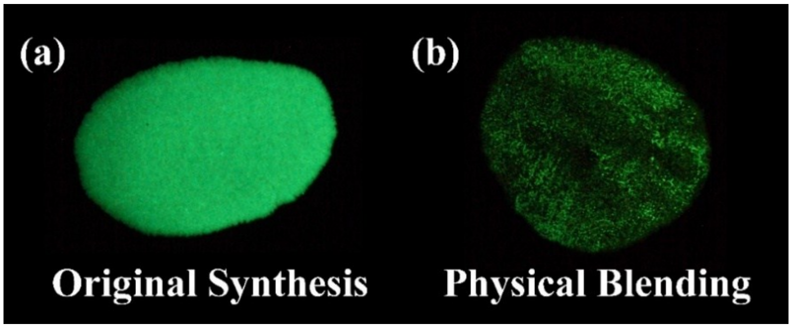

Figure S2. Photographs of afterglow emission on paper for (a) the NCD1-C ink (prepared by the synthesis method mentioned above) and (b) another reference ink (prepared by physical blending of NCD1, urea, and biuret and dispersing in DMF solution).

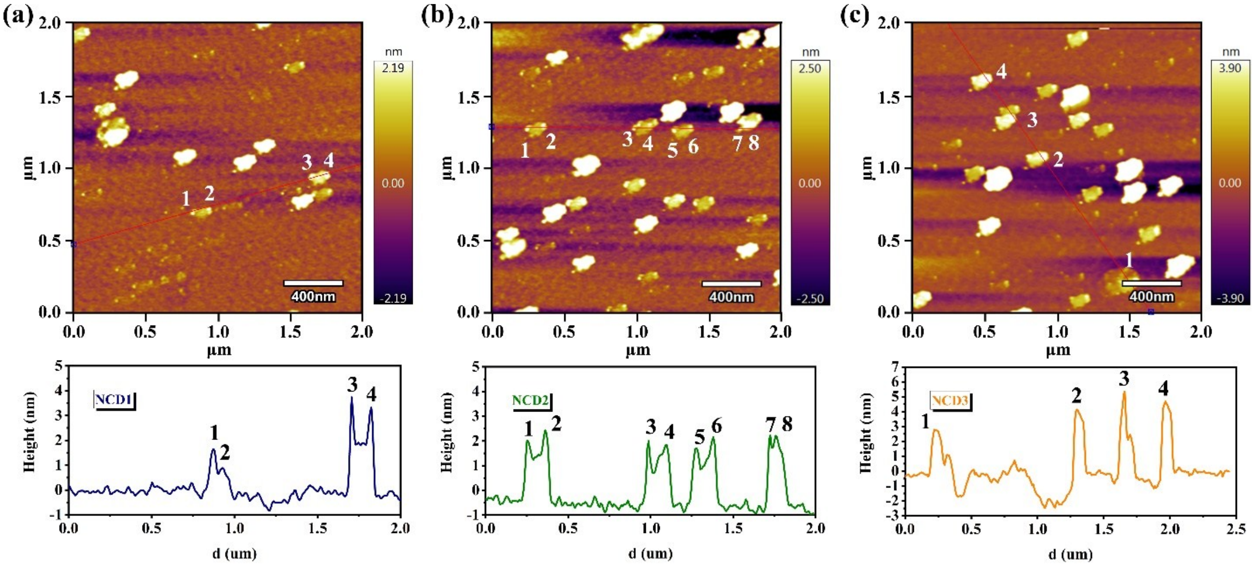

Figure S3. AFM images (top) and height profiles along the marked line (bottom) of NCD1 (a), NCD2 (b), and NCD3 (c).

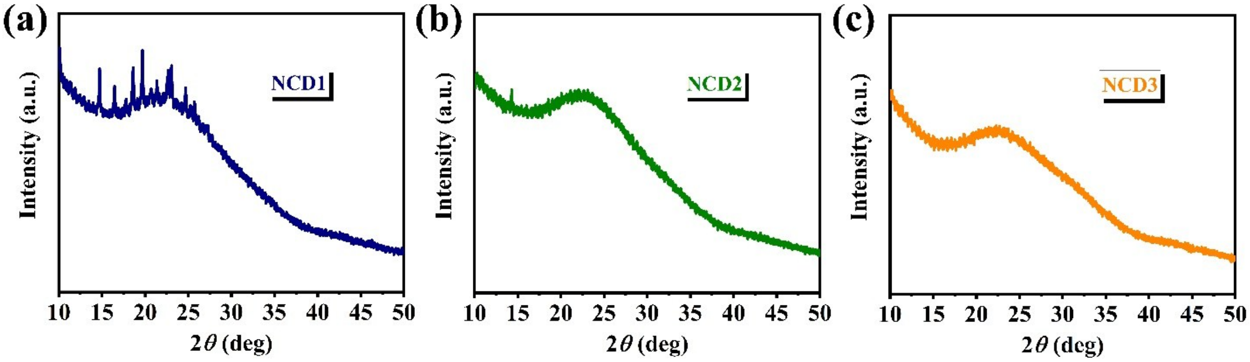

Figure S4. XRD patterns of (a) NCD1, (b) NCD2 and (c) NCD3.

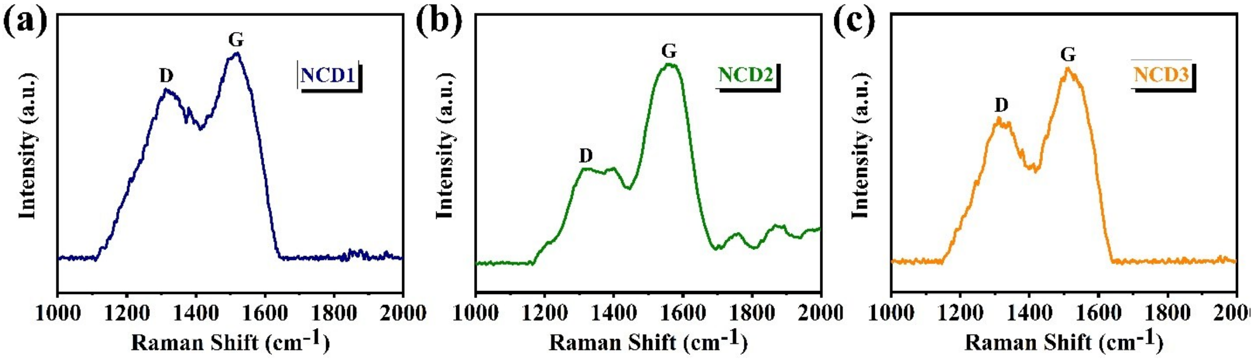

Figure S5. Raman spectra of (a) NCD1, (b) NCD2 and (c) NCD3.

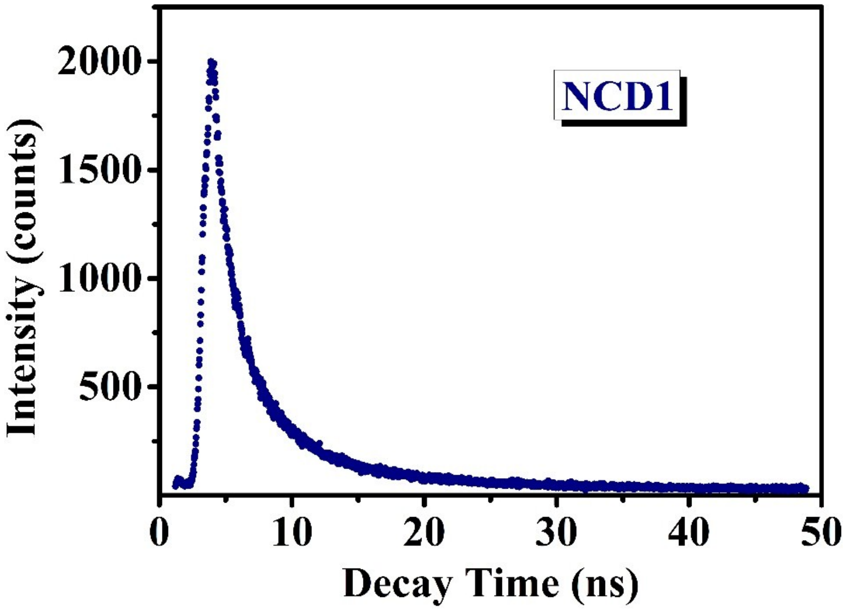

Figure S6. FL decay curve of the NCD1 in DI water. Excitation and emission wavelength were 380 nm and 450 nm, respectively.

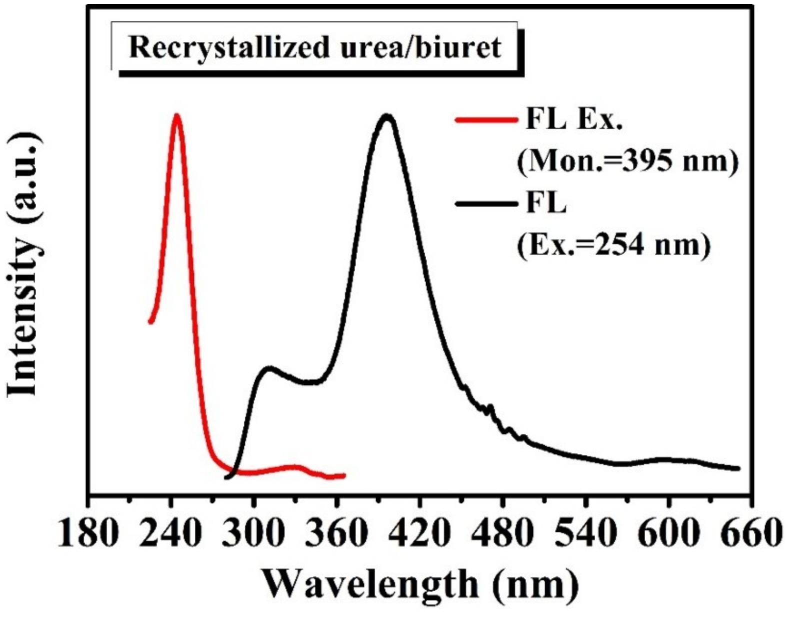

Figure S7. FL emission (black curve) and excitation (red curve) spectra of biuret/urea composites in solid state.

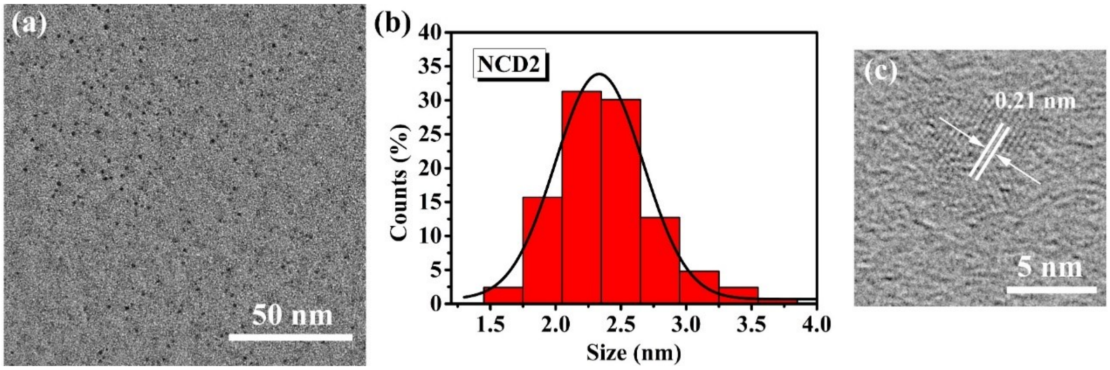

Figure S8. (a) TEM image, (b) size distribution, (c) HR-TEM image of the NCD2.

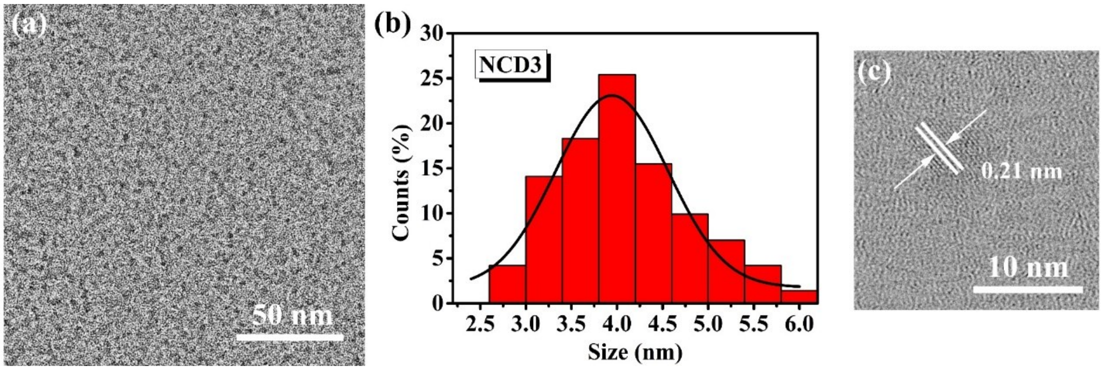

Figure S9. (a) TEM image, (b) size distribution, (c) HR-TEM image of the NCD3.

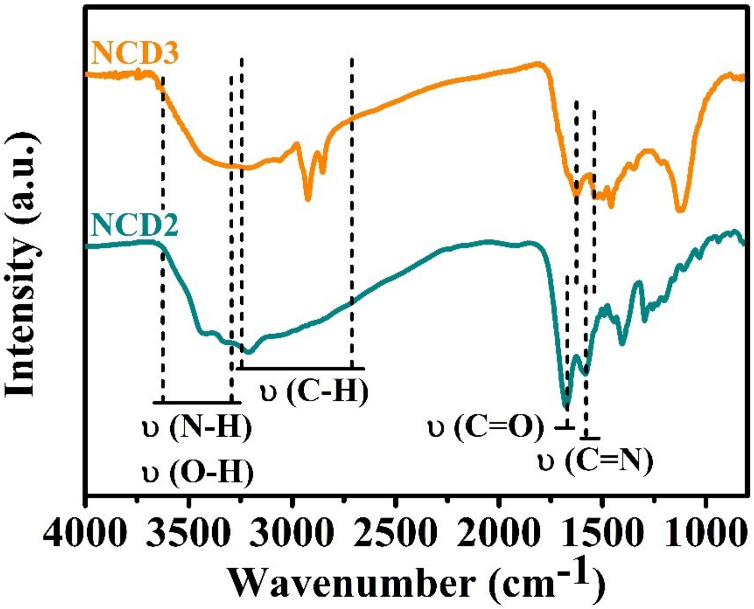

Figure S10. FT-IR spectra of the NCD2 (green curve) and NCD3 (orange curve).

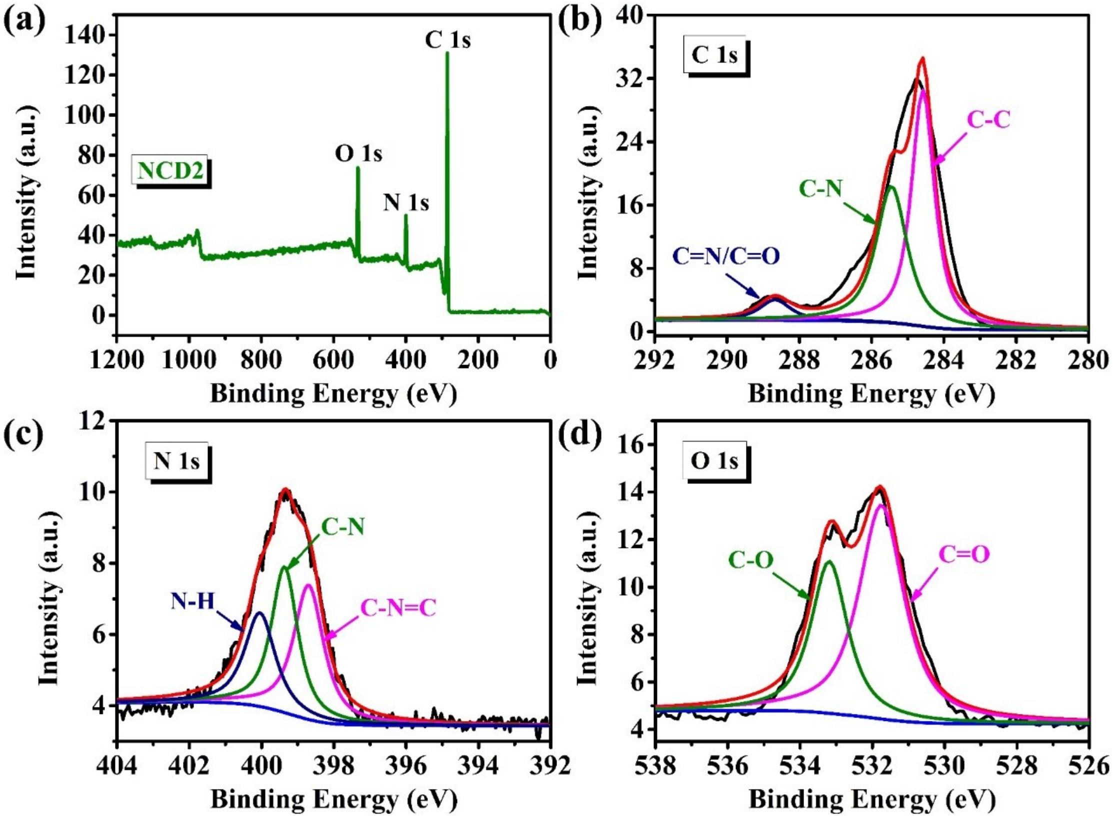

Figure S11. (a) XPS spectra and enlarged parts for (b) C 1s, (c) N 1s, (d) O 1s of the NCD2.

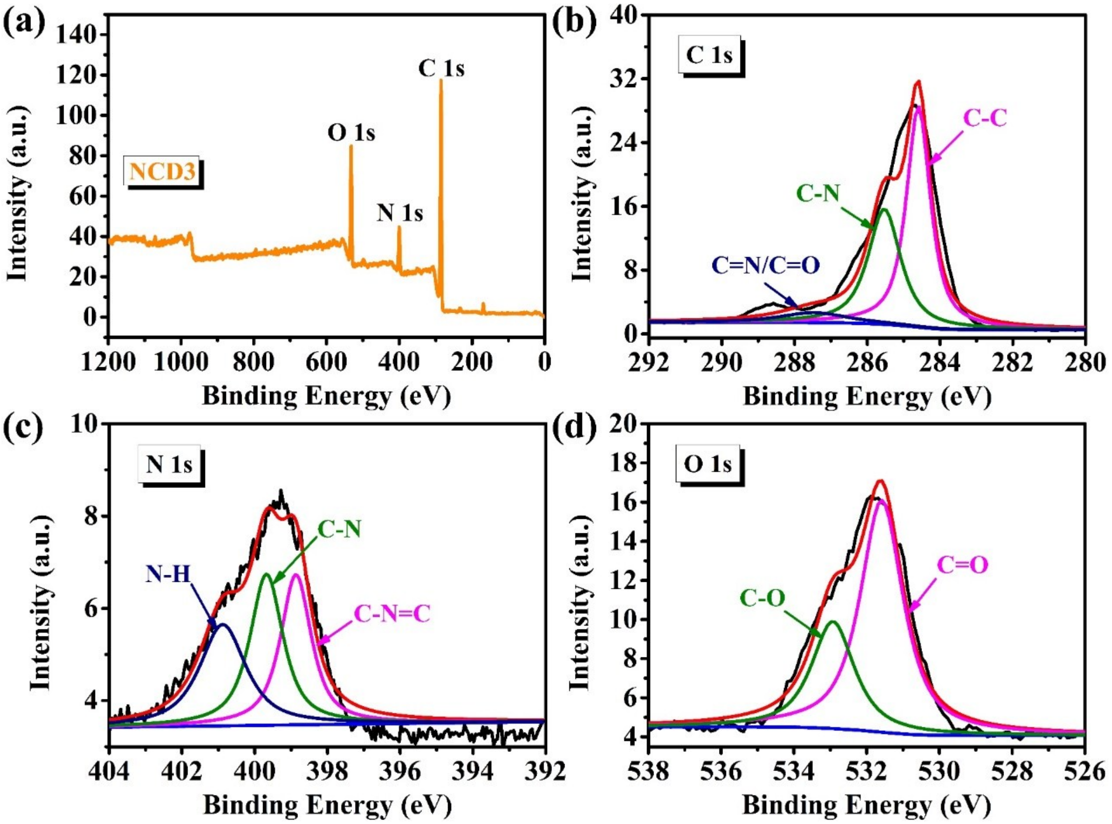

Figure S12. (a) XPS spectra and enlarged parts for (b) C 1s, (c) N 1s, (d) O 1s of the NCD3.

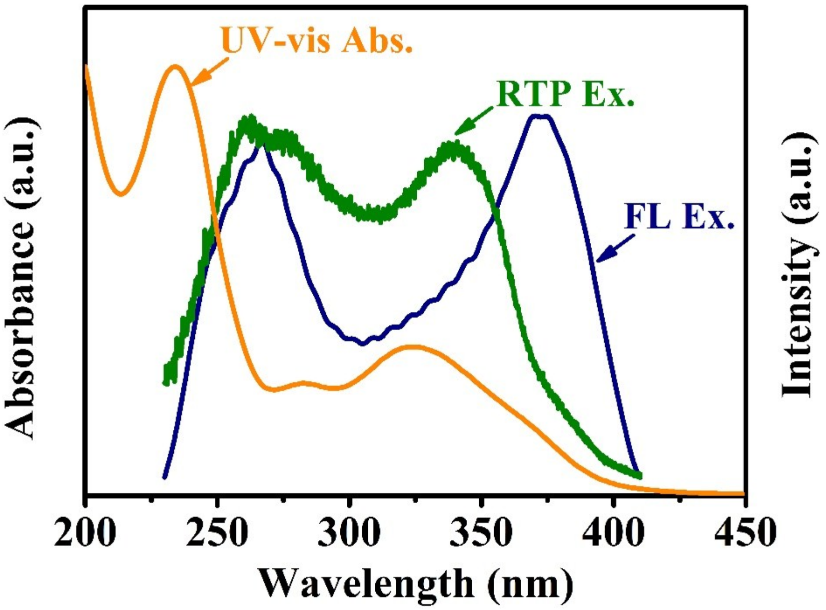

Figure S13. UV-vis absorption spectrum of the NCD2 in DI water (orange curve), FL excitation spectrum (blue curve), and RTP excitation spectrum (green curve) of the NCD2-C.

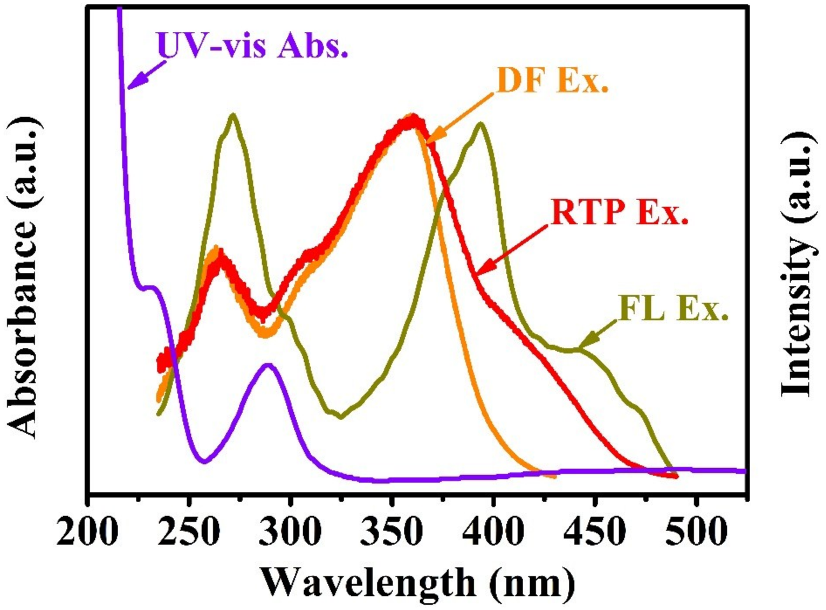

Figure S14. UV-vis absorption spectrum of the NCD3 in EtOH (purple curve), FL excitation spectrum (dark yellow curve), DF excitation spectrum (orange curve), and RTP excitation spectrum (red curve) of the NCD3-C.

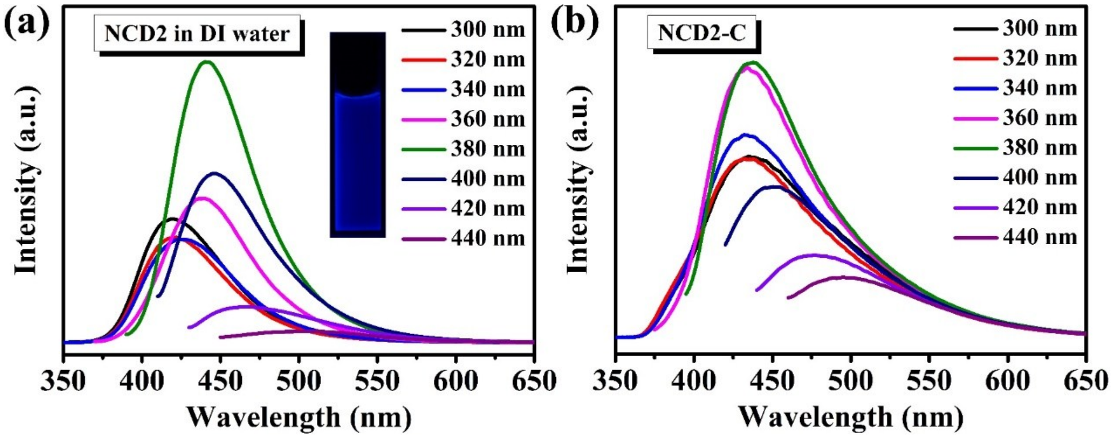

Figure S15. (a) Excitation-dependent FL spectra of the NCD2 in DI water (inset: photographs of the NCD2 solution under 365 nm irradiation). (b) Excitation-dependent FL spectra of the NCD2-C.

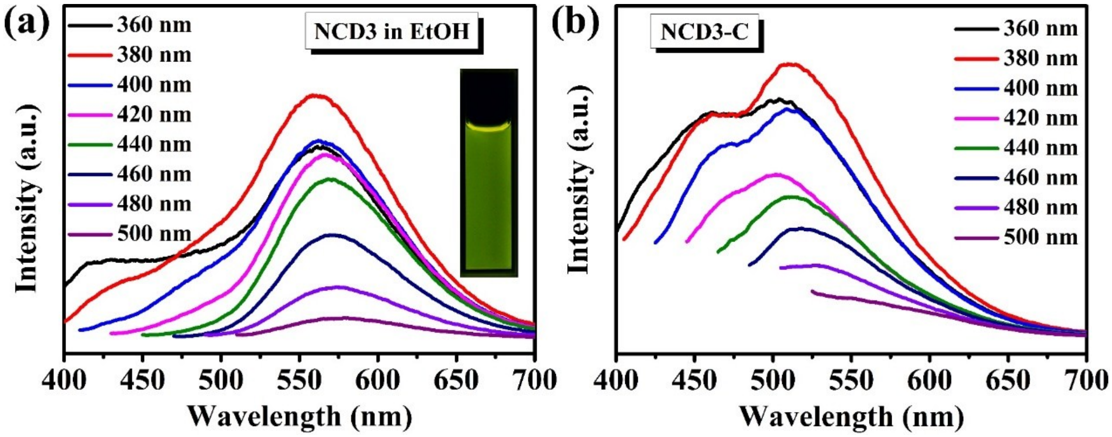

Figure S16. (a) Excitation-dependent FL spectra of the NCD3 in EtOH (inset: photograph of the NCD3 solution under 365 nm irradiation). (b) Excitation-dependent FL spectra of the NCD3-C.

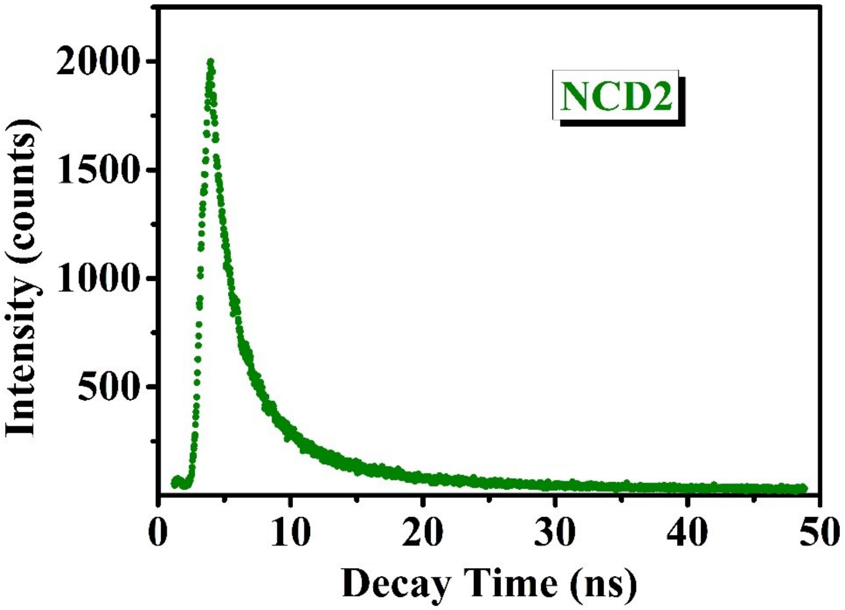

Figure S17. FL decay curve of the NCD2 in DI water (Ex. = 380 nm; Mon. = 440 nm).

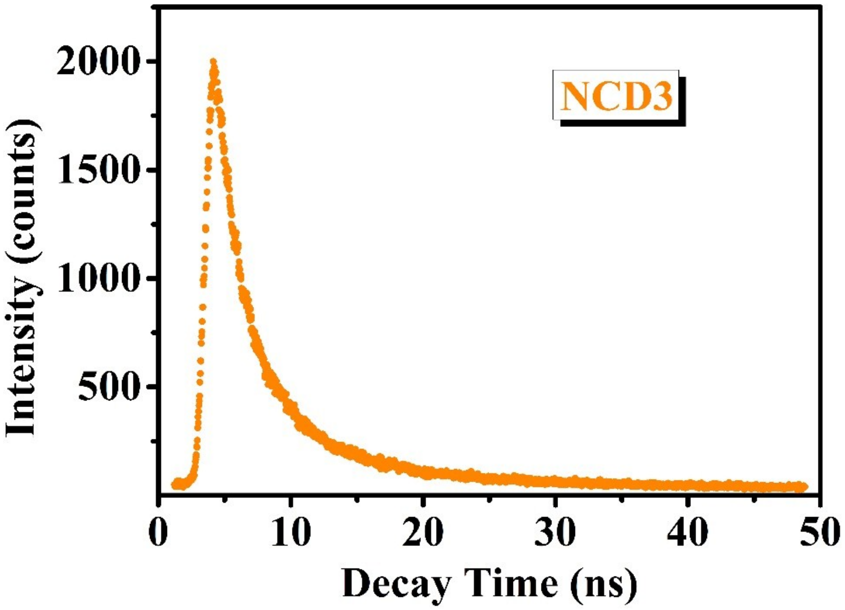

Figure S18. FL decay curve of the NCD3 in EtOH (Ex. = 380 nm; Mon. = 560 nm).

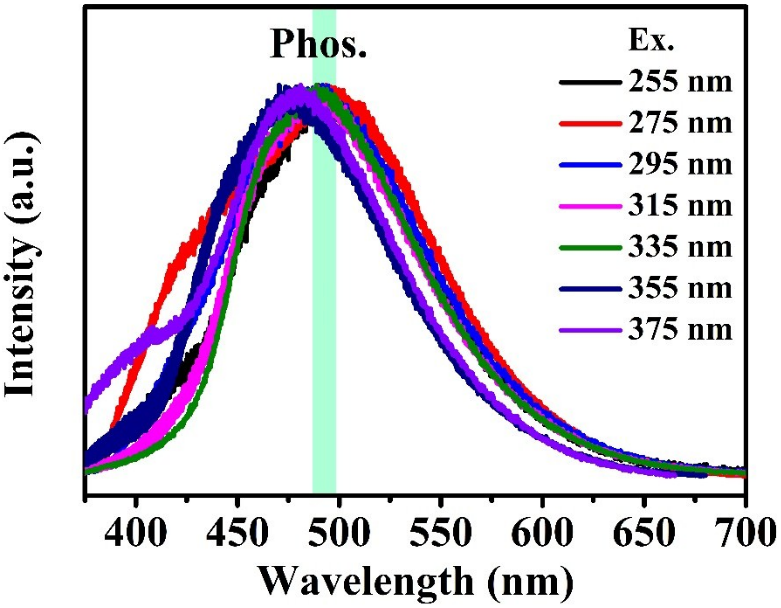

Figure S19. Afterglow emission spectra of the NCD2-C under different excitation wavelengths.

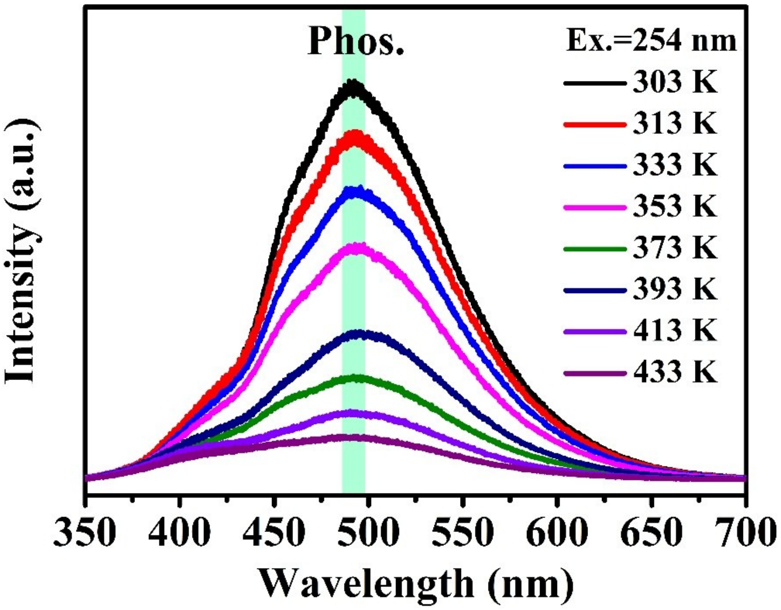

Figure S20. Afterglow emission spectra of the NCD2-C at different temperatures under 254 nm excitation.

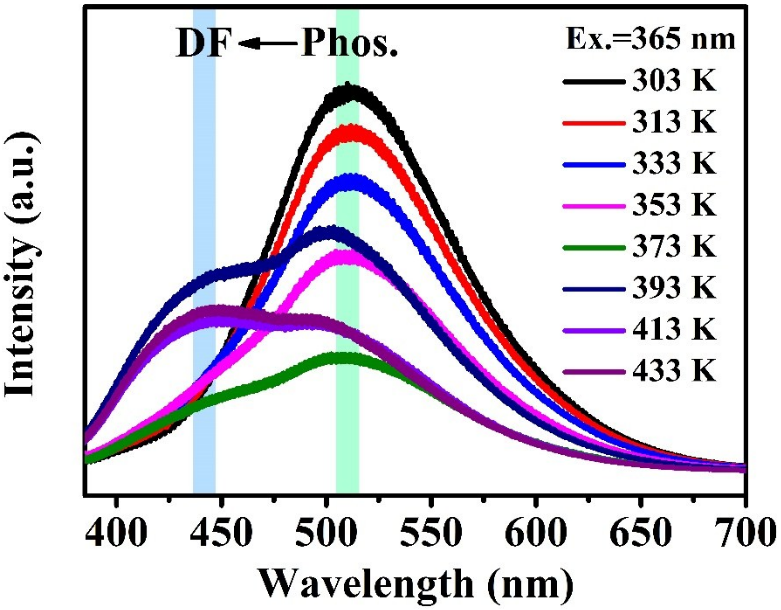

Figure S21. Afterglow emission spectra of the NCD2-C at different temperatures under 365 nm excitation.

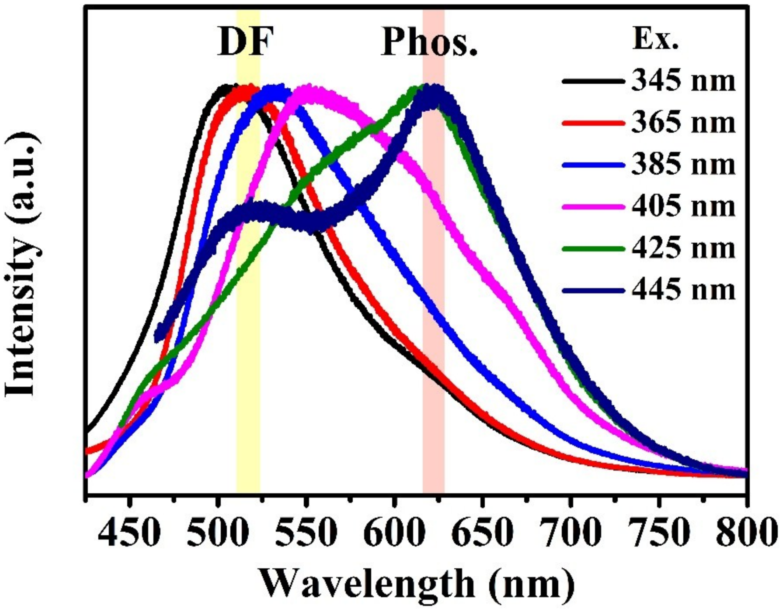

Figure S22. Afterglow emission spectra of the NCD3-C under different excitation wavelengths.

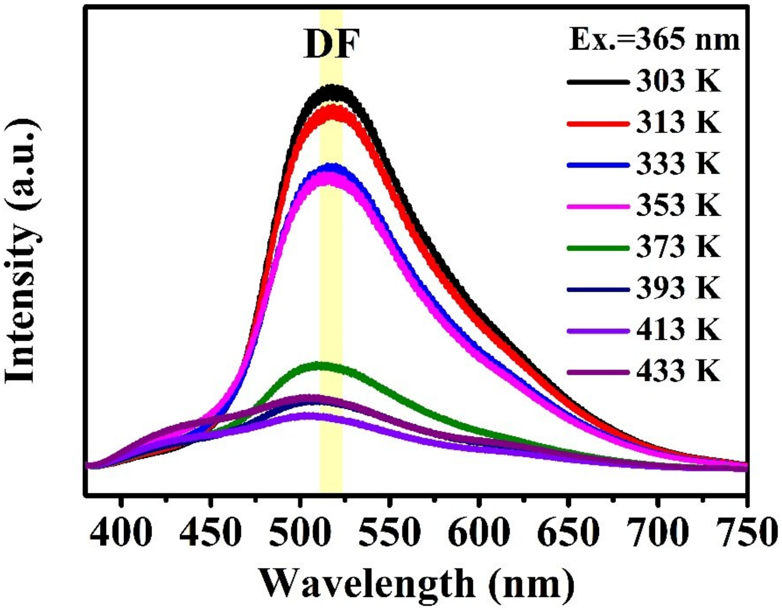

Figure S23. Afterglow emission spectra of the NCD3-C at different temperatures under 365 nm excitation.

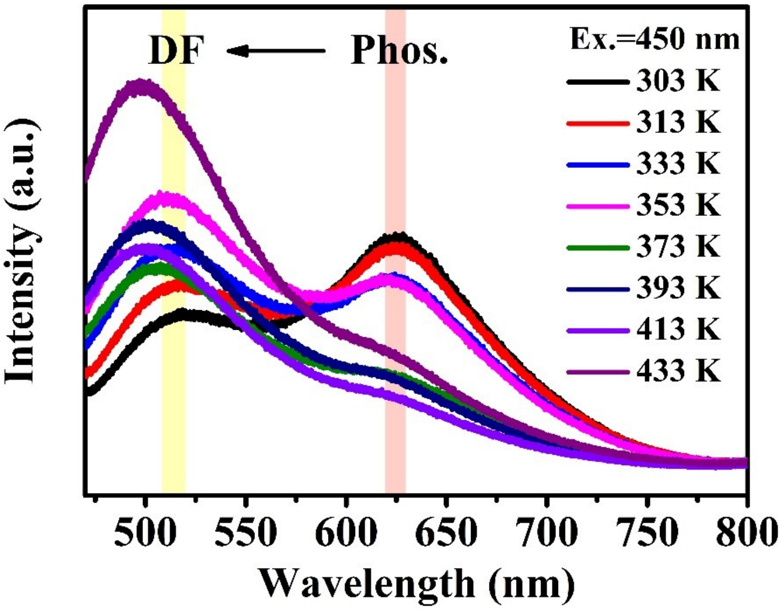

Figure S24. Afterglow emission spectra of the NCD3-C at different temperatures under 450 nm excitation.

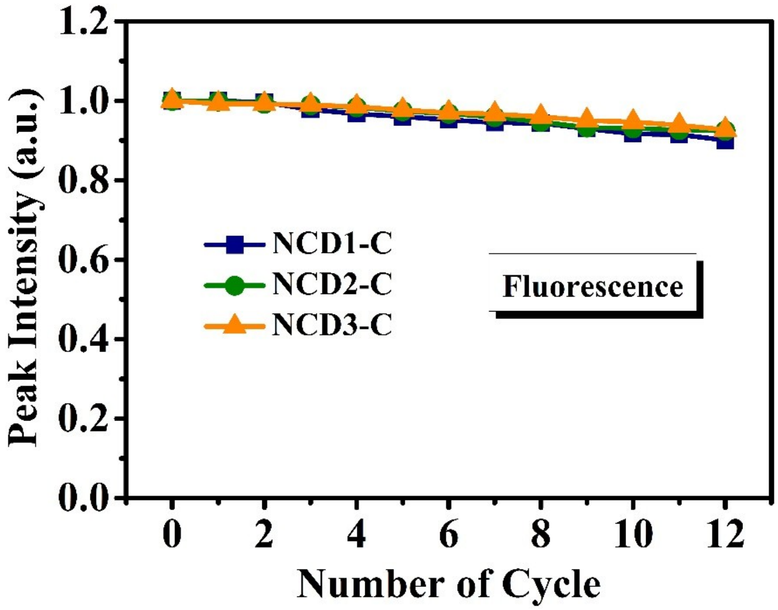

Figure S25. FL stability of the NCD1-C, NCD2-C, and NCD3-C after illumination at 254 nm for 12 times. For each time, the sample was continuously irradiated for 5 minutes. The output of the 254 nm lamp was 10V/3W.

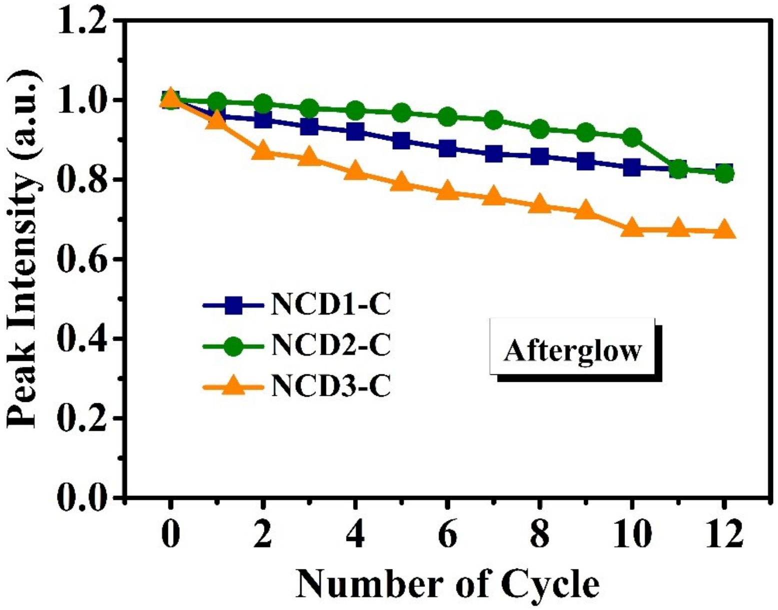

Figure S26. Afterglow stability of the NCD1-C, NCD2-C, and NCD3-C after illumination at 254 nm for 12 times. For each time, the sample was continuously irradiated for 5 minutes. The output of the 254 nm lamp was 10V/3W.

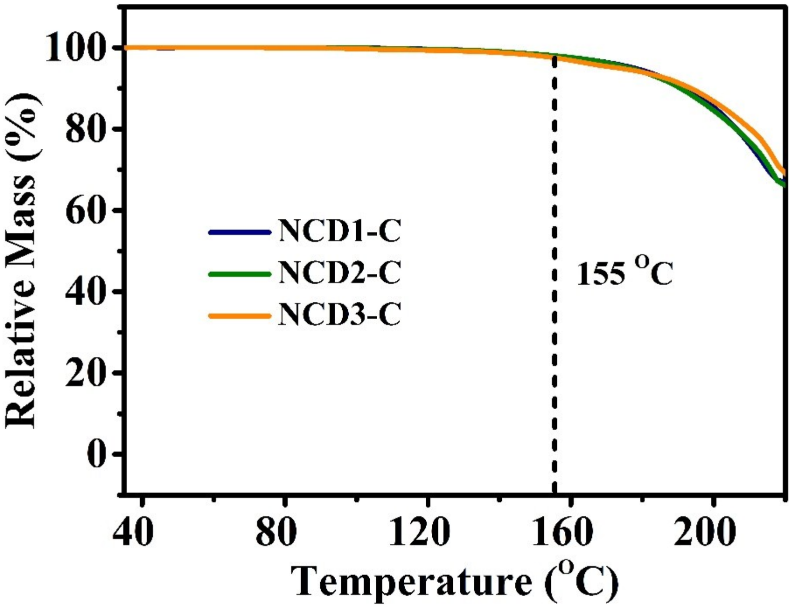

Figure S27. TGA of the NCD1-C, NCD2-C, and NCD3-C.

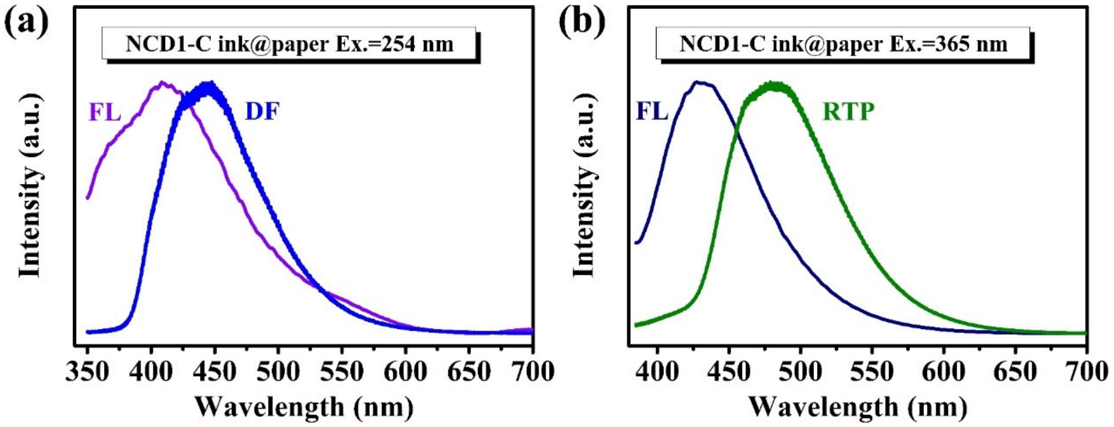

Figure S28. FL and afterglow emission spectra of the NCD1-C ink printed on paper under (a) 254 nm and (b) 365 nm excitations. The spectra were almost identical with those in NCD1-C.

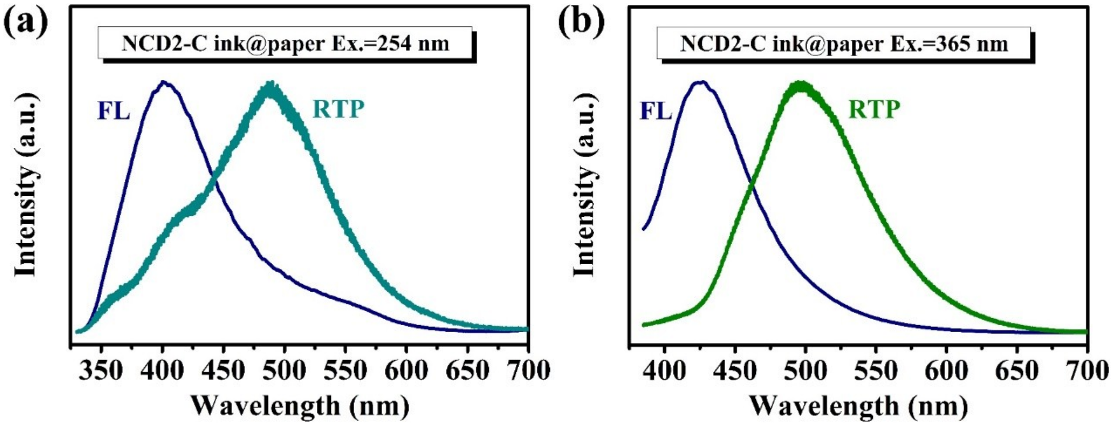

Figure S29. FL and afterglow emission spectra of the NCD2-C ink printed on paper under (a) 254 nm and (b) 365 nm excitations. The spectra were almost identical with those in NCD2-C.

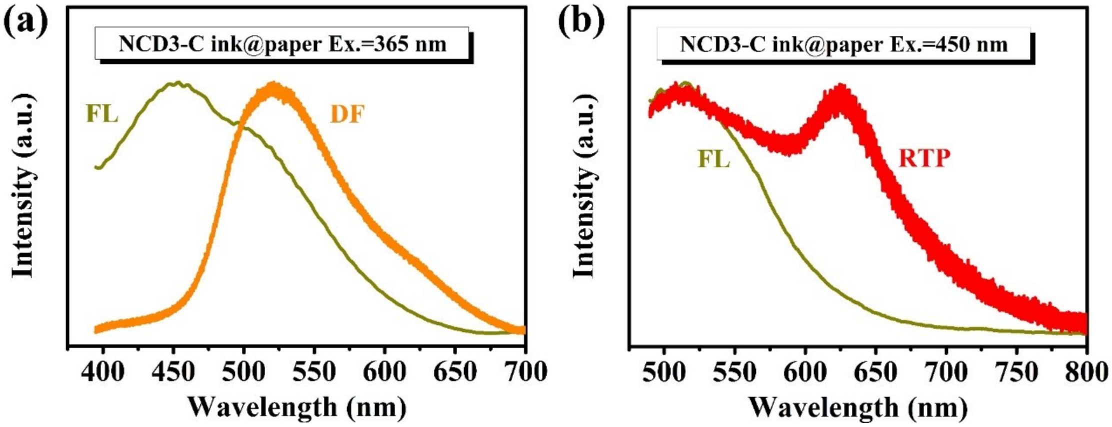

Figure S30. FL and afterglow emission spectra of the NCD3-C ink printed on paper under (a) 365 nm and (b) 450 nm excitations. The spectra were almost identical with those in NCD3-C.

Table S1. Solubility of biuret and urea in different solvents.

Solvent	Urea c (mg/mL)	Biuret c (mg/mL)	Safety
DI water	576	10	√
MeOH	11	3	√
EtOH	7	14	√
DMF	529	324	√
DMSO	1321	628	X

Table S2. Relative contents of C, O and N elements of NCD1, NCD2 and NCD3 on the basis of the XPS data.

Sample	C (%)	O (%)	N (%)
NCD1	64.3	13.9	21.8
NCD2	75.6	13.4	11.0
NCD3	73.4	15.6	11.0

Table S3. Fitted parameters of the fluorescence decay curves of NCD1, NCD2 and NCD3.

Sample	τ_1(ns)	B_1(%)	τ_2(ns)	B_2(%)	τ_{avg}(ns)	χ^2
NCD1	1.43	31705.70	5.94	1951.64	2.35	1.714
NCD2	1.37	34920.34	5.68	2096.03	2.23	1.444
NCD3	2.22	15149.91	8.43	1177.97	3.64	1.599

Table S4. Fitted parameters of the afterglow decay curves of NCD1-C.

NCD1-C	□1(ms)	B1(%)	□2(ms)	B2(%)	□3(ms)	B3(%)	□avg(ms)	□□2
Ex.=254 nm Mon.=430 nm	98.38	1.37	613.28	35.79	1254.24	62.84	1113.27	1.117
Ex.=254 nm Mon.=500 nm	23.58	3.35	293.44	19.61	1071.36	77.05	1019.78	0.994
Ex.=365 nm Mon.=500 nm	9.61	9.17	126.69	34.21	588.92	56.62	534.52	0.849

Table S5. Fitted parameters of the afterglow decay curves of NCD2-C.

NCD2-C	τ_1(ms)	B_1(%)	τ_2(ms)	B_2(%)	τ_3(ms)	B_3(%)	τ_{avg}(ms)	□χ^2
Ex.=254 nm Mon.=489 nm	49.18	8.89	321.82	32.73	1228.18	58.38	1106.47	1.001
Ex.=365 nm Mon.=502 nm	14.37	14.45	149.50	37.60	780.79	47.95	698.10	1.106

Table S6. Fitted parameters of the afterglow decay curves of NCD3-C.

NCD3-C	τ_1(ms)	B_1(%)	τ_2(ms)	B_2(%)	τ_3(ms)	B_3(%)	τ_{avg}(ms)	□χ^2
Ex.=365 nm Mon.=518 nm	25.53	7.24	253.33	44.76	919.24	48.00	780.58	0.984
Ex.=365 nm Mon.=625 nm	56.13	51.32	362.79	48.68	-	-	319.79	0.409
Ex.=450 nm Mon.=625 nm	24.50	45.85	136.23	54.15	-	-	121.46	0.202

Section V. References

1. C. Shen, Y. P. Sun, J. Wang and Y. Lu, *Nanoscale*, 2014, **6**, 9139-9147.
2. K. Jiang, S. Sun, L. Zhang, Y. Lu, A. Wu, C. Cai and H. Lin, *Angew. Chem. Int. Ed.*, 2015, **54**, 5360-5363.
3. Q. Li, M. Zhou, Q. Yang, Q. Wu, J. Shi, A. Gong and M. Yang, *Chem. Mater.*, 2016, **28**, 8221-8227.